

Testing the Standard Model in $B \rightarrow K^{(*)}\ell^+\ell^-$

Gustavo Burdman

*Fermi National Accelerator Laboratory, P. O. Box 500,
Batavia, IL 60510, U.S.A.*

Abstract

We study the potential of $B \rightarrow K^{(*)}\ell^+\ell^-$ decays as tests of the standard model. After discussing the reliability of theoretical predictions for the hadronic matrix elements involved, we examine the impact of different new physics scenarios on various observables. We show that the angular information in $B \rightarrow K^*\ell^+\ell^-$ together with the dilepton mass distribution can highly constrain new physics. This is particularly true in the large dilepton mass region, where reliable predictions for the hadronic matrix elements can be made with presently available data. We compare the Standard Model predictions with those of a Two-Higgs doublet model as well as TopColor models, all of which give distinct signals in this region.

I. INTRODUCTION

Rare decays of B mesons have a great potential as tests of the Standard Model (SM). Processes involving Flavor Changing Neutral currents (FCNC) are of particular interest given that in the SM they can only proceed via one or more loops. This leads to very small rates allowing at the same time for possible contributions from high energy scales to produce observable effects. For instance, in the SM the top quark gives a very important, and actually dominant, contribution to the process $b \rightarrow s\gamma$. Physics beyond the SM, e.g. involving new heavy particles in the loop, could contribute with comparable effects. In fact the observation by CLEO [1] of the inclusive $b \rightarrow s\gamma$ transition already constrains the parameter space of many theories [2]. On the other hand, the process $b \rightarrow s\ell^+\ell^-$ involves additional information on FCNC and is an important complement to $b \rightarrow s\gamma$ in testing the SM. Although there is still no observation of any of these modes, the experimental situation looks very promising both at e^+e^- [4] as well as hadronic machines [5]. Unlike in $b \rightarrow s\gamma$, where there are no reliable ways to calculate the hadronic matrix elements in exclusive modes (e.g. $B \rightarrow K^*\gamma$), the corresponding quantities in $B \rightarrow K^{(*)}\ell^+\ell^-$ can be safely predicted with the help of heavy quark symmetry [3]. The fact that these exclusive modes can be theoretically clean together with the additional information resulting from a richer kinematics, make these decays very interesting both theoretically as well as experimentally. While $b \rightarrow s\gamma$ proceeds via only one operator, the $b \rightarrow s\ell^+\ell^-$ processes receive contributions from two additional operators at the weak scale. This will imply that the information on higher energy scales, encoded in the coefficients of these operators, not only affects the rates but also the shape of the dilepton mass and angular distributions. These features have been recently pointed out by several authors [6–8]. In this paper we clarify some the issues related to the extraction of hadronic matrix elements in $B \rightarrow K^{(*)}\ell^+\ell^-$ and also show explicitly how different signals probe distinct aspects of the theories beyond the SM. In particular we show the effects of a class of models in which the new physics couples preferentially to the third generation [9]. In these type of scenarios, the large mass of the top quark is explained by new gauge interactions that are strong with the third generation, but rather weak with the first two. As a consequence, the first low energy test of these models is in B decays, with the $B \rightarrow K^{(*)}\ell^+\ell^-$ modes the most sensitives. In Sec. II we present the short distance structure of $b \rightarrow s\ell^+\ell^-$. We emphasize the distinction between theories that respect the SM operator basis and those that expand it. This will prove to be relevant when studying the phenomenology of $B \rightarrow K^{(*)}\ell^+\ell^-$ decays. In Sec. III we review the relations predicted

by heavy quark symmetry that allow reliable predictions of $B \rightarrow K^{(*)} \ell^+ \ell^-$ decays in terms of experimental information from other modes. In Sect. IV we show the predictions of the SM, a Two-Higgs doublet extension of it and of TopColor models, in order to compare the signals of these different scenarios. We conclude in Sec. V.

II. SHORT DISTANCE STRUCTURE

In the SM the diagrams contributing to $b \rightarrow s \ell^+ \ell^-$ processes are shown in Fig. 1. It is convenient to write down an effective theory at low energies by integrating out the heavy degrees of freedom. These are the W boson and top quark inside the loops in Fig. 1. In general, in theories beyond the SM there will be additional contributions. The effective hamiltonian can be written as an operator product expansion as

$$H_{\text{eff}} = \frac{4}{\sqrt{2}} G_F V_{tb}^* V_{ts} \sum_i C_i(\mu) O_i(\mu) \quad (1)$$

where $\{O_i(\mu)\}$ is the relevant operator basis and the $C_i(\mu)$ are the corresponding coefficient functions which must cancel the dependence on the energy scale μ . The dimension six operator basis is, in the SM [10,11]

$$\begin{aligned} O_1 &= (\bar{s}_\alpha \gamma_\mu b_{L\alpha}) (\bar{c}_\beta \gamma^\mu c_{L\beta}) & O_6 &= (\bar{s}_\alpha \gamma_\mu b_{L\beta}) \sum_q (\bar{q}_\beta \gamma^\mu q_{R\alpha}) \\ O_2 &= (\bar{s}_\alpha \gamma_\mu b_{L\beta}) (\bar{c}_\beta \gamma^\mu c_{L\alpha}) & O_7 &= \frac{e^2}{16\pi^2} m_b (\bar{s} \sigma_{\mu\nu} b_R) F^{\mu\nu} \\ O_3 &= (\bar{s}_\alpha \gamma_\mu b_{L\alpha}) \sum_q (\bar{q}_\beta \gamma^\mu q_{L\beta}) & O_8 &= \frac{e^2}{16\pi^2} (\bar{s} \gamma_\mu b_L) (\bar{\ell} \gamma^\mu \ell) \\ O_4 &= (\bar{s}_\alpha \gamma_\mu b_{L\beta}) \sum_q (\bar{q}_\beta \gamma^\mu q_{L\alpha}) & O_9 &= \frac{e^2}{16\pi^2} (\bar{s} \gamma_\mu b_L) (\bar{\ell} \gamma^\mu \gamma_5 \ell) \\ O_5 &= (\bar{s}_\alpha \gamma_\mu b_{L\alpha}) \sum_q (\bar{q}_\beta \gamma^\mu q_{R\beta}) \end{aligned} \quad (2)$$

where $q_{L,R} = \frac{(1 \mp \gamma_5)}{2} q$ and α, β are color indices. The coefficients at $\mu = m_b$ are obtained when their values at $\mu = M_W$ are evolved using the renormalization group equation. This has been done in a partial leading logarithmic approximation in [10] for the SM as well as for Two-Higgs doublet models. The complete leading logarithmic approximation for the SM has been recently computed in [12]. For the purpose of this paper it is sufficient to make use

of the approximation in [10], given that the uncertainties related to long distance dynamics, even when reduced by symmetry arguments (see next section), are still larger than the error made by using it. For a complete discussion see [13]. The short distance information is then encoded in the $C_i(M_W)$'s. Several theories beyond the SM share this operator basis with it. Their extra contributions at the electroweak or higher energy scales appear as changes in the values of the coefficients at $\mu = M_W$. There are also theories that require an extension of the operator basis. For instance, the chirality of the quark currents could be reversed, giving

$$O'_7 = \frac{e^2}{16\pi^2} m_b (\bar{s} \sigma_{\mu\nu} b_L) F^{\mu\nu} \quad (3a)$$

$$O'_8 = \frac{e^2}{16\pi^2} (\bar{s} \gamma_\mu b_R) (\bar{\ell} \gamma^\mu \ell) \quad (3b)$$

$$O'_9 = \frac{e^2}{16\pi^2} (\bar{s} \gamma_\mu b_R) (\bar{\ell} \gamma^\mu \gamma_5 \ell) \quad (3c)$$

as well as the ones resulting from $b_L \rightarrow b_R$ in $O_1 - O_6$.

The SM, supersymmetry, multi-Higgs models and most technicolor scenarios only modify the value of the short distance coefficients $C_i(M_W)$, without inducing additional operators. On the other hand, left-right symmetric models, compositeness and topcolor are among the theories capable of inducing sizeable wrong-chirality contributions as well as shifts in the normal-chirality coefficients. These two very different groups of electroweak symmetry breaking scenarios are likely to give drastically different signals, for instance for the angular distributions. The only operator entering in $b \rightarrow s\gamma$ at the weak scale is O_7 . Therefore, radiative processes have a rather limited power as SM tests: only the shifts induced in $C_7(M_W)$ are probed. Conversely, $b \rightarrow s\ell^+\ell^-$ processes are more sensitive to new physics which might give small or null deviations of the $b \rightarrow s\gamma$ rate but still give large contributions to the other coefficients in (1). These would produce not only a different rate but also distinct patterns in the dilepton mass distributions as well as the angular distributions.

III. RELIABLE PREDICTIONS FOR $B \rightarrow K^{(*)}\ell^+\ell^-$

The use of experimental information in $b \rightarrow s\ell^+\ell^-$ processes requires the theoretical understanding of hadronic effects. The inclusive rate $B \rightarrow X_s\ell^+\ell^-$ is theoretically clean in this

respect and can be predicted with rather low uncertainties [6,14]. However, its experimental observation might prove to be a very difficult task. On the other hand, exclusive modes like $B \rightarrow K\ell^+\ell^-$ and $B \rightarrow K^*\ell^+\ell^-$ are more accesible to both e^+e^- and hadronic machines, but the need to compute hadronic matrix elements of the operators in (2) and (3) introduces potentially large hadronic uncertainties. The situation appears to be similar to the one in $B \rightarrow K^*\gamma$, where the large disagreement among model calculations of the matrix element of O_7 between B and K^* renders this mode almost useless as a test of the SM. However, in the present case these large uncertainties can be avoided by making use of Heavy Quark Symmetry (HQS), which relates the hadronic matrix elements entering in $B \rightarrow K^{(*)}\ell^+\ell^-$ decays to those entering in semileptonic decays [3]. It must be emphasized that we *do not* consider the limit in which the s quark is heavy, as is done in part of previous work on these decays. In the rest of this section we review the implementation of these relations and make use of them in $b \rightarrow s\ell^+\ell^-$ exclusive decays.

A. $B \rightarrow K^*\ell^+\ell^-$

As we will see below, this mode is the most interesting one from the phenomenological point of view. We need the matrix elements of the operators O_7 , O_8 , O_9 , O'_7 , O'_8 and O'_9 . The hadronic matrix elements of O_7 and O'_7 can be written as

$$\begin{aligned} \langle K^*(k) | \bar{s} \sigma_{\mu\nu} (1 \pm \gamma_5) b | B(P) \rangle &= \epsilon_{\mu\nu\alpha\beta} \left\{ A \epsilon^{*\alpha} P^\beta + B \epsilon^{*\alpha} k^\beta + C \epsilon^* . P P^\alpha k^\beta \right\} \\ &\quad \pm i \left\{ A (\epsilon^{*\mu} P^\nu - \epsilon^{*\nu} P^\mu) + B (\epsilon^{*\mu} k^\nu - \epsilon^{*\nu} k^\mu) \right. \\ &\quad \left. + C \epsilon^* . P (P^\mu k^\nu - P^\nu k^\mu) \right\} \end{aligned} \quad (4)$$

where A , B and C are unknown functions of $q^2 = (P - k)^2$, the squared momentum transferred to the leptons. On the other hand, the matrix elements of the semileptonic operators O_8 , O_9 , O'_8 and O'_9 are parametrized by

$$\begin{aligned} \langle K^*(k) | \bar{s} \gamma_\mu (1 \pm \gamma_5) b | B(P) \rangle &= i g \epsilon_{\mu\nu\alpha\beta} \epsilon^{*\nu} (P + k)^\alpha (P - k)^\beta \\ &\quad \pm f \epsilon_\mu^* \pm a_+ \epsilon^* . P (P + k)_\mu \pm a_- \epsilon^* . P (P - k)_\mu \end{aligned} \quad (5)$$

with g , f and a_\pm also unknown functions of q^2 .

In the Heavy Quark Limit, where the mass of the b quark is infinitely heavy compared to the typical scale of the strong interactions, the Dirac structure of (4) is related to that of

(5). The simplification arises because in the $m_b \gg \Lambda_{\text{QCD}}$ limit the heavy quark spinor loses its two lower components becoming

$$b(x) \approx \begin{pmatrix} \Psi(x) \\ 0 \end{pmatrix} \quad (6)$$

That is, the two lower components are suppressed by m_b . As a consequence, the action of gamma matrices on the b spinor simplifies. One has, for instance $\gamma_0 b = b$. The $(0i)$ component of (4) is now related to the (i) component of (5) by the relations

$$i\sigma_{0i} = \gamma_i \quad (7)$$

$$i\sigma_{0i}\gamma_5 = -\gamma_i\gamma_5$$

By making use of (7) we can obtain now relations among the form-factors in (4) and (5). They are [3]

$$A = \frac{-f + 2m_B k_0 g}{m_B} \quad (8a)$$

$$B = -2m_B g \quad (8b)$$

$$C = \frac{a_+ - a_- + 2g}{m_B} \quad (8c)$$

Furthermore, the semileptonic $B \rightarrow K^*$ form-factors g , f and a_{\pm} are identical to the $B \rightarrow \rho\ell\nu$ form-factors in the $SU(3)$ limit. Therefore, the hadronic matrix elements entering in $B \rightarrow K^*\ell^+\ell^-$ are given by the $B \rightarrow \rho\ell\nu$ form-factors to leading order in Λ_{QCD}/m_b and in the $SU(3)$ limit. In this way, experimental information on $B \rightarrow \rho\ell\nu$ can be used as a prediction for $B \rightarrow K^*\ell^+\ell^-$. The relations (8) can be also used to predict the $B \rightarrow K^*\gamma$ rate. In this case, however the region of the $B \rightarrow \rho\ell\nu$ Dalitz plot that can be used is negligibly small. This is due the fact that one needs the semileptonic form-factors evaluated at $q^2 = 0$ in the case with a real photon. Moreover, the ρ must be left-handed in order to have the same combination of form-factors that appear in the radiative decay. Both conditions can only be satisfied in one corner, corresponding to the ρ and the charged lepton having both maximum momenta. The rate at this point vanishes due to phase space, and thus an extrapolation

to this point must be made in order to extract a model independent quantity that would constitute the $B \rightarrow K^* \gamma$ hadronic matrix element [15]. The situation is very different here. We are able to use all the $B \rightarrow \rho \ell \nu$ Dalitz plot, which in the SU(3) limit covers exactly the $B \rightarrow K^* \ell^+ \ell^-$ Dalitz plot.

Presently, there are only upper limits for $B \rightarrow \rho \ell \nu$ [16]. However the observation of $B \rightarrow \pi \ell \nu$ at CLEO [16] indicates that there will be data on this mode very soon. We can make use of present data by taking an extra step in using the heavy quark symmetries. This time we use the flavor symmetry that relates processes with b and c quark hadrons. This implies relations among the semileptonic $B \rightarrow K^*$ form-factors entering in (5) and those in the decay $D \rightarrow K^* \ell \nu$. Up to a short-distance correction factor, these relations are the simple mass scaling laws [3]:

$$f^B(v.k) = \sqrt{\frac{m_B}{m_D}} f^D(v.k) \quad (9a)$$

$$g^B(v.k) = \sqrt{\frac{m_D}{m_B}} g^D(v.k) \quad (9b)$$

$$(a_+ - a_-)^B(v.k) = \sqrt{\frac{m_D}{m_B}} (a_+ - a_-)^D(v.k) \quad (9c)$$

where the form-factors in the left-hand side of (9) are those in $B \rightarrow K^* \ell^+ \ell^-$ and those in the right-hand side those entering in $D \rightarrow K^* \ell \nu$. The relations (9) are valid when the form-factors are evaluated at the same value of $v.k$, with v the heavy meson four-velocity and k_μ the K^* four-momentum. In the rest frame of the heavy meson this is the K^* recoil energy, E_{K^*} . Thus, we can only predict $B \rightarrow K^* \ell^+ \ell^-$ for values of E_{K^*} ranging from m_{K^*} to the maximum recoil in $D \rightarrow K^* \ell \nu$. In terms of $q^2 = m_{\ell\ell}^2$, the dilepton invariant mass squared, this implies the window $4.0\text{GeV} < m_{\ell\ell} < 4.4\text{GeV}$, where the upper value is actually the maximum allowed dilepton mass. Model independent predictions for the $B \rightarrow K^* \ell^+ \ell^-$ form-factors for smaller dilepton masses will only be possible when the $B \rightarrow \rho \ell \nu$ data is available. We will make use of the form-factors extracted in $D \rightarrow K^* \ell \nu$ decays [17] to illustrate how the SM predictions compare with those of some of its extensions.

In order to take full advantage of the information provided by this decay we first notice that the amplitude can be divided into two non-interfering pieces corresponding to left and

right-handed leptons. Each of them can then be expressed as a sum of helicity amplitudes. The squared amplitude is

$$\left| A \left(B \rightarrow K^* \ell^+ \ell^- \right) \right|^2 = |H_+^L|^2 + |H_-^L|^2 + |H_+^R|^2 + |H_-^R|^2 + |H_0|^2 \quad (10)$$

where the $L(R)$ refer to left (right)-handed leptons and the subindices \pm and 0 indicate the transverse and longitudinal polarizations of the K^* . When the heavy quark relations (8) are imposed, the helicity amplitudes depend only on the semileptonic form-factors f , g and a_+ . The transverse helicities take the form

$$\begin{aligned} H_\alpha^L = & - \left[C_7 \frac{m_b (m_B - E_* + \eta_\alpha \mathbf{k})}{q^2} + \frac{C_8 - C_9}{2} \right] (f + \eta_\alpha 2m_B \mathbf{k}g) \\ & + \left[C_7' \frac{m_b (m_B - E_* - \eta_\alpha \mathbf{k})}{q^2} + \frac{C_8' - C_9'}{2} \right] (f - \eta_\alpha 2m_B \mathbf{k}g) \end{aligned} \quad (11a)$$

$$\begin{aligned} H_\alpha^R = & - \left[C_7 \frac{m_b (m_B - E_* + \eta_\alpha \mathbf{k})}{q^2} + \frac{C_8 + C_9}{2} \right] (f + \eta_\alpha 2m_B \mathbf{k}g) \\ & + \left[C_7' \frac{m_b (m_B - E_* - \eta_\alpha \mathbf{k})}{q^2} + \frac{C_8' + C_9'}{2} \right] (f - \eta_\alpha 2m_B \mathbf{k}g) \end{aligned} \quad (11b)$$

where $\alpha = +, -$ and $\eta_a = (1, -1)$. The longitudinal helicity is

$$\begin{aligned} H_0 = & \frac{m_{B^2}}{2m_{K^*}\sqrt{q^2}} \left\{ -2(C_7 - C_7') \frac{m_b}{q^2 m_B} \left[f(m_B E_* - m_{K^*}^2) + 2m_B^2 \mathbf{k}^2 g \right] \right. \\ & \left. + \frac{(C_8 - C_9 - C_8' + C_9')}{2} \left[4\mathbf{k}^2 a_+ - \frac{2E_*}{m_B} f \right] \right\} \end{aligned} \quad (12)$$

In (11) and (12) E_* and \mathbf{k} are the energy and spatial momentum of the K^* in the B rest frame, the short distance coefficients must be evaluated at $\mu = m_b$ and the form-factors at $q^2 = m_{\ell\ell}^2$. The latter can be either the semileptonic form-factors extracted from $B \rightarrow \rho \ell \nu$ or, by applying (9), those from $D \rightarrow K^* \ell \nu$. One can immediately see from (11) that there is an interesting interplay between the short distance coefficients and the combination of form-factors entering in each transverse helicity. For instance, the first term in each of (11a) and (11b) corresponds to the contributions from normal-helicity operators, whereas the second line comes from the one with wrong chirality. Depending on the sign η_α , some contributions

will be enhanced and some suppressed by the form-factors. This will lead to rather distinct signals when considering different physics scenarios at M_W or higher scales.

The angular information is most sensitive to the details of the helicity amplitudes. The forward-backward asymmetry for leptons was considered in the contexts of both inclusive [6] and exclusive [8] $b \rightarrow s\ell^+\ell^-$ processes. Defining θ_ℓ as the polar angle formed by the ℓ^+ and the B meson in the $\ell^+\ell^-$ rest frame, the double differential decay rate has the form

$$\frac{d^2\Gamma}{dq^2 d\cos\theta_\ell} = \frac{G_F^2 \alpha^2 |V_{tb}^* V_{ts}|^2}{768\pi^5 m_B^2} kq^2 \left\{ (1 + \cos\theta_\ell)^2 [|H_+^L|^2 + |H_-^R|^2] \right. \\ \left. (1 - \cos\theta_\ell)^2 [|H_-^L|^2 + |H_+^R|^2] + 2\sin^2\theta_\ell |H_0|^2 \right\} \quad (13)$$

Then the forward-backward asymmetry is defined by

$$A_{FB}(q^2) = \frac{\int_0^1 \frac{d^2\Gamma}{dq^2 d\cos\theta_\ell} dq^2 - \int_{-1}^0 \frac{d^2\Gamma}{dq^2 d\cos\theta_\ell} dq^2}{\int_0^1 \frac{d^2\Gamma}{dq^2 d\cos\theta_\ell} dq^2 + \int_{-1}^0 \frac{d^2\Gamma}{dq^2 d\cos\theta_\ell} dq^2} \quad (14)$$

which, making use of (13), gives

$$A_{FB} = \frac{3}{4} \frac{|H_-^L|^2 + |H_+^R|^2 - |H_+^L|^2 - |H_-^R|^2}{|H_-^L|^2 + |H_+^R|^2 + |H_+^L|^2 + |H_-^R|^2 + |H_0|^2} \quad (15)$$

Alternatively, one can simply use the angular distribution. In the next section we present results for the asymmetry and the dilepton mass distributions in several theories, including the SM.

B. $B \rightarrow K\ell^+\ell^-$

We now turn to the pseudoscalar decay mode. The hadronic matrix elements of the operators O_i and O'_i , $i = 7, 8, 9$, are now

$$\langle K(k) | \bar{s} \sigma_{\mu\nu} b | B(P) \rangle = D [(P+k)_\mu (P-k)_\nu - (P+k)_\nu (P-k)_\mu] \quad (16)$$

$$\langle K(k) | \bar{s} \gamma_\mu b | B(P) \rangle = f_+(P+k)_\mu + f_-(P-k)_\mu \quad (17)$$

with D , and f_\pm unknown functions of $q^2 = m_{\ell\ell}^2$. Using (7) one obtains

$$D = -\frac{(f_+ - f_-)}{2m_B} \quad (18)$$

In the SU(3) limit f_{\pm} are the $B \rightarrow \pi \ell \nu$ form-factors. Measurements of this mode already exist [16] but are still not precise enough. On the other hand the flavor heavy quark symmetry predicts [3]

$$(f_+ - f_-)^B(v.k) = \sqrt{\frac{m_B}{m_D}}(f_+ - f_-)^D(v.k) \quad (19)$$

where the B and the D labels refer to the $B \rightarrow K \ell^+ \ell^-$ and $D \rightarrow K \ell \nu$ decays respectively. The window in which a reliable prediction for $B \rightarrow K \ell^+ \ell^-$ can be obtained from the charm semileptonic decay data is now $4.2\text{GeV} < m_{\ell\ell} < 4.8\text{GeV}$. The dilepton mass distribution takes the form

$$\frac{d\Gamma}{dq^2} = \frac{G_F^2 |V_{tb}^* V_{ts}|^2 \alpha^2 \mathbf{k}^2}{192\pi^5} \left\{ |(C_8 + C'_8)f_+ - 2Dm_b(C_7 + C'_7)|^2 + |(C_9 + C'_9)f_+|^2 \right\} \quad (20)$$

From (20) it can be seen that the chirality of the operators is not tested in this mode. It is not possible to distinguish a shift in the coefficients of the normal operator basis from a non-zero value of the “wrong” chirality operators in (3). The information of this decay could be, however, an important complement to $B \rightarrow K^* \ell^+ \ell^-$.

IV. PREDICTIONS

In this section we consider various Electroweak Symmetry Breaking Scenarios and their signals in $B \rightarrow K^{(*)} \ell^+ \ell^-$ decays. The main purpose is to illustrate the potential of these rare decays to discriminate among theories. The results presented here make use of the form-factor relations (8) and (9). The use of the latter implies a restriction of the theoretically safe predictions to the region with $m_{\ell\ell} > 4.0\text{GeV}$ in the $B \rightarrow K^* \ell^+ \ell^-$ case. We slightly extend this region down to 3.8 GeV to cover the dilepton mass region above the Ψ' background from the indirect process $B \rightarrow K^* \Psi' \rightarrow K^* \ell + \ell^-$. For the $B \rightarrow K \ell^+ \ell^-$ case we present results for the region $4.2\text{GeV} < m_{\ell\ell} < 4.8\text{GeV}$, which is allowed by the use of $D \rightarrow K \ell \nu$ data in (19).

A. Standard Model

At the electroweak scale the only operators contributing to the $b \rightarrow s \ell^+ \ell^-$ transitions are O_7 , O_8 and O_9 . However, when evolved down to the b quark scale, they mix with O_1 and O_2 . The coefficients at $\mu = M_W$ are [18]

$$C_7(M_W) = \frac{1}{2}A(x) \quad (21)$$

$$C_8(M_W) = \frac{B(x)}{s^2\theta_w} + \frac{4s^2\theta_w - 1}{s^2\theta_w}C(x) + D(x) - \frac{4}{9} \quad (22)$$

$$C_9 = -\frac{B(x)}{s^2\theta_w} + \frac{C(x)}{s^2\theta_w} \quad (23)$$

where $x = (m_t^2/M_W^2)$ and with

$$A(x) = \frac{x}{(x^3 - 1)} \left\{ \frac{2}{3}x^2 + \frac{5}{12}x - \frac{7}{12} - \frac{x(3/2x - 1)}{(x - 1)} \ln x \right\} \quad (24)$$

$$B(x) = \frac{x}{4(x - 1)} \left\{ \frac{1}{(x - 1)} \ln x - 1 \right\} \quad (25)$$

$$C(x) = \frac{x}{4(x - 1)} \left\{ \frac{x}{2} - 3 + \frac{(3/2x^2 + 1)}{(x - 1)} \ln x \right\} \quad (26)$$

$$D(x) = \frac{1}{(x^3 - 1)} \left\{ \frac{25}{36}x^2 - \frac{19}{36}x^3 + \frac{\left(-\frac{x^4}{6} + \frac{5}{3}x^3 - 3x^2 + \frac{16}{9}x - \frac{4}{9}\right)}{(x - 1)} \ln x \right\} \quad (27)$$

We also need $C_1(M_W) = 0$ and $C_2(M_W) = -1$. Defining $\eta = \alpha_s(m_b)/\alpha_s(M_W)$, the evolution to m_b gives [10]

$$C_7(m_b) = \eta^{-16/23} \left\{ C_7(M_W) - \frac{58}{135} \left(\eta^{10/23} - 1 \right) C_2(M_W) - \frac{29}{189} \left(\eta^{28/23} - 1 \right) C_2(M_W) \right\}, \quad (28)$$

$$\begin{aligned} C_8(m_b) = C_8(M_W) + \frac{4\pi}{\alpha_s(M_W)} & \left\{ \frac{4}{33} \left(\eta^{-11/23} - 1 \right) \right. \\ & \left. + \frac{8}{27} \left(1 - \eta^{-29/23} \right) \right\} C_2(M_W) + [C_1(m_b) + C_2(m_b)] g(m_c/m_b; q^2) \end{aligned} \quad (29)$$

where

$$C_{1,2}(m_b) = \frac{1}{2} \left[\eta^{-6/23} \mp \eta^{12/23} \right] C_2(M_W) \quad (30)$$

and the last term in $C_8(m_b)$ comes from the one-loop contributions of O_1 and O_2 , which gives a dependence on q^2 . For $q^2 > 4m_c^2$ it is given by the function

$$g(z, s) = - \left\{ \frac{4}{9} \ln z^2 - \frac{8}{27} - \frac{16}{9} \frac{z^2}{s} + \frac{2}{9} \sqrt{1 - \frac{4z^2}{s^2}} \left(2 + \frac{4z^2}{s^2} \right) \left[\ln \left| \frac{1 + \sqrt{1 - \frac{4z^2}{s^2}}}{1 - \sqrt{1 - \frac{4z^2}{s^2}}} \right| + i\pi \right] \right\} \quad (31)$$

where the imaginary part arises when the charm quarks in the loop go on shell. In calculating the asymmetry and dilepton mass distribution we do not include the long distance pieces coming from the $B \rightarrow K^* J/\Psi$ plus $J/\Psi \rightarrow \ell^+ \ell^-$ or the analogous process for the Ψ' . The limitations from using $D \rightarrow K^* \ell \nu$ data keep our predictions at $m_{\ell\ell}$ above these contributions.

We are now in the position of calculating the forward-backward asymmetry for leptons and the dilepton mass distribution in the SM. We use $m_t = 175$ GeV for the evaluation of the short-distance coefficients and we take $|V_{tb}^* V_{ts}| \approx s^2 \theta_c$. As it can be seen in Fig. 2(a), the SM has a large and negative A_{FB} . This is due to the fact that the largest helicity amplitude is $|H_+^L|$. The right-handed lepton amplitudes are negligible, mostly due to cancellations among short-distance coefficients, whereas $|H_-^L|$ is suppressed by the combination of form-factors entering in (11a) with $\eta_- = 1$. The dilepton mass distribution is shown in Fig. 3(a).

B. Two-Higgs Doublet Model

As a first extension of the minimal SM we consider an extension in the Higgs sector. In models with two Higgs doublets, tree level flavor changing neutral currents are avoided by coupling quarks of the same charge to the same Higgs doublet. One such model corresponds to the up quarks getting their masses from one scalar doublet and the down quarks from the other. The resulting coupling of the charged Higgs to quarks implies a new contribution to the loop in Fig. (1) by replacing the W with the charged Higgs. These contributions have been extensively studied in the literature [10,11]. They effectively shift the values of the short distance coefficients C_7 , C_8 and C_9 at $\mu = M_W$. We choose to study the Model II in the notation of Ref. [10], which corresponds to the Higgs sector of the minimal supersymmetric standard model. Its short distance coefficients are given by

$$C_7(M_W) = \frac{1}{2} A(x) + G(y) + \frac{1}{6} \left(\frac{v_2}{v_1} \right)^2 A(x) \quad (32)$$

where

$$G(y) = \frac{y}{2(y-1)^2} \left[\frac{5}{6} y - \frac{1}{2} - \frac{(y-2/3)}{(y-1)} \ln y \right] \quad (33)$$

with $x = m_t^2/M_W^2$ and $y = m_t^2/m_h^2$. The coefficients C_8 and C_9 at the electroweak scale are

$$C_8(M_W) = \frac{B(x)}{s^2\theta_w} + \frac{4s^2\theta_w - 1}{s^2\theta_w} \left[C(x) - \left(\frac{v_2}{v_1} \right) \frac{x}{2} B(y) \right] \\ + D(x) - \frac{4}{9} + \frac{v_2}{v_1} y F(y) \quad (34)$$

$$C_9(M_W) = -\frac{B(x)}{s^2\theta_w} + \frac{1}{s^2\theta_w} \left[C(x) - \left(\frac{v_2}{v_1} \right)^2 \frac{x}{2} B(y) \right] \quad (35)$$

with

$$F(y) = \frac{1}{(y-1)^3} \left[\frac{47}{108} y^2 - \frac{79}{108} y + \frac{19}{54} + \frac{(y/3 - y^3/6 - 2/9)}{(y-1)} \ln y \right] \quad (36)$$

On the other hand, extending the Higgs sector does not give contributions to operators outside the SM operator basis (2). The coefficients C'_7 , C'_8 and C'_9 corresponding to the operators in (3) remain zero. The model is determined by the value of m_h , the charged Higgs mass, and $\tan\beta = v_2/v_1$, the ratio of vacuum expectation values of the two Higgs doublets. For instance, for $m_h = 200\text{GeV}$ and $\tan\beta = 1$ the A_{FB} in this model is given by the dotted line in Fig. 2(a). The asymmetry is reduced with respect to its SM value. The comparison to the SM dilepton mass distribution can be seen in Fig. 3(a).

C. TopColor Models

We now turn to a class of models that has the potential to give not only sizeable shifts in the coefficients C_7 , C_8 and C_9 but also can generate contributions to “wrong” chirality operators. Non-zero values of C'_7 , C'_8 and C'_9 strongly affect the pattern of helicities with respect to the SM. This can be clearly appreciated from the expression (11) for the transverse helicities, where the terms containing the “wrong”-chirality coefficients are multiplied by the combination of form-factors with the opposite relative sign. This implies, for instance, that H_-^L could become comparable to H_+^L , which would induce a cancellation in A_{FB} . Right-handed helicities could also become important.

TopColor models [9] are of interest due to the fact that they give special status to the third generation through the dynamical generation of the top quark mass. The dynamics at $\approx 1\text{TeV}$ is given by the gauge structure

$$SU(3)_1 \times U(1)_{Y_1} \times SU(3)_2 \times U(1)_{Y_2} \rightarrow SU(3)_{\text{QCD}} \times U(1)_Y \quad (37)$$

The $SU(3)_1 \times U(1)_{Y_1}$ couples strongly to the third generation whereas the $SU(3)_2 \times U(1)_{Y_2}$ is strongly coupled to the first two. The $SU(3)_1 \times U(1)_{Y_1}$ is assumed to be strong enough to

form a chiral $\langle t\bar{t} \rangle$ condensate, but not $\langle b\bar{b} \rangle$ or $\langle \tau\bar{\tau} \rangle$ condensates, giving a large mass to the top quark. There is a residual $SU(3)' \times U(1)'$ which implies the existence of a massive color octet B_μ^a (topgluon) and a singlet Z'_μ . The couplings of the latter to the quarks are given by [9]

$$\begin{aligned} \mathcal{L}_{Z'} = Z'_\mu g_1 \left\{ \tan \theta' \left(\frac{1}{3} \bar{\psi}_L \gamma_\mu \psi_L + \frac{4}{3} \bar{u}_R \gamma_\mu u_R - \frac{2}{3} \bar{d}_R \gamma_\mu d_R \right) \right. \\ \left. - \cot \theta' \left(\frac{1}{3} \bar{\chi}_L \gamma_\mu \chi_L + \frac{4}{3} \bar{t}_R \gamma_\mu t_R - \frac{2}{3} \bar{b}_R \gamma_\mu b_R \right) \right\} \end{aligned} \quad (38)$$

where $\psi = (u, d)$, $\chi = (t, b)$ and g_1 is the $U(1)_Y$ coupling. The angle θ' is small, which selects the top quark direction for condensation. The corresponding Z'_μ coupling to first and second generation leptons is also suppressed by $\tan \theta'$, whereas the coupling to the τ lepton is enhanced by $\cot \theta'$. After rotation to the mass eigenstates, (38) generates four-fermion interactions leading to additional contributions to the $b \rightarrow s \ell^+ \ell^-$ transitions. For $\ell = e, \mu$, the short-distance coefficients are independent of θ' and are given by

$$C_8 = C_8^{SM} + \frac{1}{2} \kappa \frac{V_{bs}}{V_{tb} V_{ts}^*} \quad (39a)$$

$$C_9 = C_9^{SM} + \frac{1}{6} \kappa \frac{V_{bs}}{V_{tb} V_{ts}^*} \quad (39b)$$

and, for the coefficients of (3)

$$C'_8 = -\kappa \frac{W_{bs}}{V_{tb} V_{ts}^*} \quad (40a)$$

$$C'_9 = -\frac{1}{3} \kappa \frac{W_{bs}}{V_{tb} V_{ts}^*} \quad (40b)$$

where we have defined

$$\kappa = \frac{8\pi^2 v^2}{M_{Z'}^2} \left(\frac{M_Z}{M_W} \right)^2 \quad (41)$$

and $V_{bs} = D_{bs}^{*L} D_{bb}^L$ and $W_{bs} = D_{bs}^{*R} D_{bb}^R$ are the residual non-diagonal terms in the Z' couplings after the diagonalization of the mass matrix for down-type quarks according to $D^{L\dagger} M_D D^R$.

The FCNC couplings V_{bs} and W_{bs} are only fixed by a specific realization of the model. In order to make a prediction, we take them to be equal and approximately half the SM charged current equivalent V_{ts} (The squared root ansatz in [9]).

$$|V_{bs}| \approx |W_{bs}| \approx \pm \frac{1}{2} |V_{ts}| \quad (42)$$

The results for the asymmetry are plotted in Fig. 2(b) for the minus sign in (42) and for both $M_{Z'} = 500\text{GeV}$ and $M_{Z'} = 1\text{TeV}$. In both cases, but in particular in one of them, it can be seen that the asymmetry is very different than the one obtained in the SM. The dilepton mass distributions are shown in Fig. 3(b). The effect of the Z' is striking both in the asymmetry and the dilepton mass distribution, even when looking at such a restricted region of phase space. The asymmetry becomes a more sensitive test for a much heavier Z' . For instance for $M_{Z'} = 1\text{TeV}$ the branching ratio is not much larger than in the SM, whereas the asymmetry is still significantly different. In Table I we show the branching ratios and asymmetries corresponding to $m_{\ell\ell} > 3.8\text{GeV}$ in the cases considered above.

We finally point out that TopColor models as the ones considered above, that produce observable effects with $\ell = e$ and μ are likely to give very large effects for $\ell = \tau$. This is due to the fact that the four-fermion interactions induced by (38) together with the similar Lagrangian for τ leptons, are proportional to $\cot^2 \theta'$. This implies large contributions to $b \rightarrow s\tau^+\tau^-$ processes like $B \rightarrow K^{(*)}\tau^+\tau^-$ and $B_s \rightarrow \tau^+\tau^-$ [19].

The results for $B \rightarrow K\ell^+\ell^-$ can be seen in Fig. 4, where the dilepton mass distributions are plotted for the various cases considered above and in the region allowed by the use of the relations (19). It can be seen that this mode is not such a powerful test of the SM. However its observation will be an important complement to the information extracted from $B \rightarrow K^*\ell^+\ell^-$. The results for this decay are summarized in Table II.

V. CONCLUSIONS

As we have seen in previous sections, the decay $B \rightarrow K^*\ell^+\ell^-$ is a powerful test of the SM. This is true even when the present experimental situation restricts the reliable predictions of hadronic matrix elements to the region with $m_{\ell\ell}^2 > m_{\Psi}^2$. The angular information is likely to be an extremely useful tool given its sensitivity to changes in the short distance coefficients in (1). The forward-backward asymmetry A_{FB} is very large and negative in the SM, as it can be seen in Fig. 2(a) and in Table I. This is caused by an accidental partial cancellation

in the short-distance factor that makes the helicity H_+^L to be significantly larger than all the others, causing a large negative value in (15).

On the other hand, the Two-Higgs doublet scenario we discussed in Sect. IV, with $\tan \beta = 1$ and $m_h = 200$ GeV, gives a considerably smaller asymmetry even when the dilepton mass distribution is not very different from that of the SM (Fig. 3(a)).

We have also considered the effects of TopColor models [9]. The $b \rightarrow s\ell^+\ell^-$ decays are the first low energy data that could be strongly affected by the phenomenology of these models, which are also expected to produce important effects on top and bottom production [20] as well as on $\Gamma(Z \rightarrow b\bar{b})$ [21]. We have seen in Sect. IV that a 500 GeV color-singlet boson strongly coupled to the third generation gives large deviations from the SM in both the asymmetry and the dilepton mass distribution, as long as the neutral mixing induced is chosen to be of the same order as the corresponding CKM matrix element as in (42). The asymmetry (Fig. 2(b), dashed line) is largely reduced with respect to the SM value. This is due not only to shifts in the coefficients C_8 and C_9 which upset the cancellation taking place in the SM, but also due to non-zero values of C'_8 and C'_9 , the coefficients of the “wrong” chirality operators O'_8 and O'_9 in (3). The latter implies important contributions to helicity amplitudes that were largely suppressed in the SM. The sensitivity of the angular information to non-zero values of these coefficients is illustrated in the case $m_{Z'} = 1$ TeV. There, the dilepton mass distribution (Fig. 3(b), dotted-dash line) is not very different from the SM prediction. However, the asymmetry is still substantially smaller, as can be appreciated from Fig. 2(b).

Although it is true that reliable predictions for the hadronic matrix elements are presently limited to large dilepton masses, this might not be such an important limitation regarding the quality of the angular information. The availability of $B \rightarrow \rho\ell\nu$ data will allow SM tests for all dilepton masses in $B \rightarrow K^*\ell^+\ell^-$. However the distinctive features of the angular information are likely to disappear or not be so important for smaller $m_{\ell\ell}^2$. For instance, the SM asymmetry will not be so large for smaller $m_{\ell\ell}^2$ due to the absence of a near cancellation in some of the short distance factors in (11). This suggests that concentrating on the region of large $m_{\ell\ell}^2$ is not just convenient because of the lack of information from $B \rightarrow \rho\ell\nu$, but also because the angular information is most discriminating there. The pseudoscalar mode $B \rightarrow K\ell^+\ell^-$ is not as rich in information as $B \rightarrow K^*\ell^+\ell^-$ is, but it can be a powerful complement to it. For instance, the Two-Higgs doublet model considered here gives slightly larger rates in both modes, whereas the TopColor model that gives the largest rate in $B \rightarrow K^*\ell^+\ell^-$ produces a rate in $B \rightarrow K\ell^+\ell^-$ that is *smaller* than in the SM, as can be seen

in Table II.

In the near future experiments in both hadron and e^+e^- colliders will have sensitivity to branching fractions as the ones in Tables II and II. The current upper limit corresponds to a partial branching fraction in the region we have considered, of approximately $(1 - 2) \times 10^{-5}$ [4,5] for the $B \rightarrow K^*\ell^+\ell^-$ mode. Therefore, experimental information is about to start constraining new physics models and soon will be at the level of the SM predictions. The reconstruction of the dilepton asymmetries will then be an important probe into the physics of the electroweak symmetry breaking scale.

ACKNOWLEDGMENTS

The author thanks Marcia Begalli, Gerhard Buchalla, Fritz De Jongh and Chris Hill for useful suggestions and comments. This work was supported by the U.S. Department of Energy.

TABLES

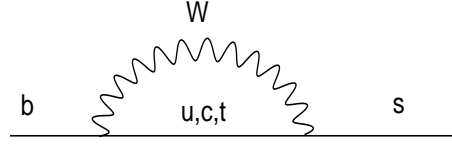
	$a_{FB}^{partial}$	$B.R.^{partial}(\times 10^{-6})$
SM	-0.57	0.53
2HD	-0.35	0.64
TopC ($M_{Z'} = 500\text{GeV}$)	-0.138/ - 0.250	4.0/5.0
TopC ($M_{Z'} = 1 \text{ TeV}$)	-0.36/ - 0.46	0.6/0.9

TABLE I. Integrated asymmetry and branching fraction in the region $m_{\ell\ell} > 3.8\text{GeV}$ in $B \rightarrow K^*\ell^+\ell^-$. For TopColor we take into account both possible relative signs ($-/+$) between the FCNC couplings and the corresponding CKM matrix elements.

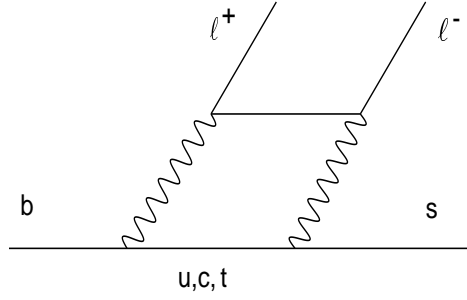
	$B.R.^{partial}(\times 10^{-7})$
SM	1.6
2HD	1.9
TopC ($M_{Z'} = 500\text{GeV}$)	1.1/2.5
TopC ($M_{Z'} = 1 \text{ TeV}$)	0.6/1.0

TABLE II. Integrated branching fraction in the region $m_{\ell\ell} > 4.2\text{GeV}$ in $B \rightarrow K\ell^+\ell^-$. For TopColor we take into account both possible relative signs ($-/+$) between the FCNC couplings and the corresponding CKM matrix elements.

FIGURES



(a)



(b)

FIG. 1. Diagrams contributing to $b \rightarrow s \ell^+ \ell^-$.

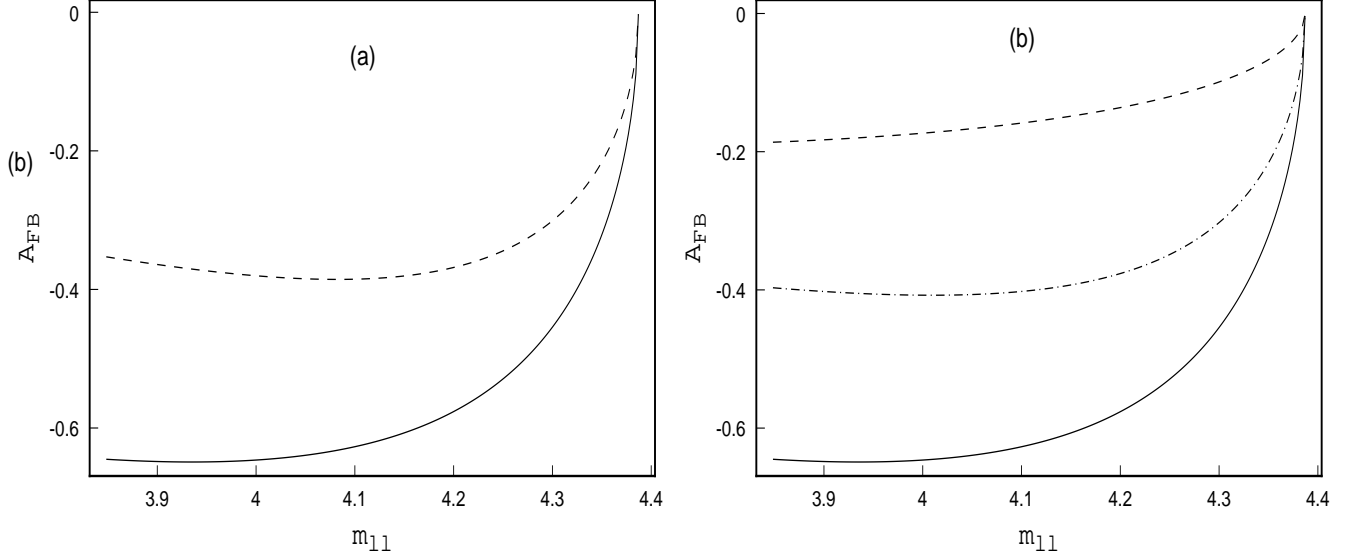


FIG. 2. Forward-Backward asymmetry for leptons as a function of the dilepton mass in $B \rightarrow K^* \ell^+ \ell^-$. The solid line is the SM prediction. In (a), the dashed line is the Two-Higgs doublet model. In (b), the dashed line is the Top-Color prediction for $m_{Z'} = 500$ GeV, whereas the dotted-dashed line corresponds to $m_{Z'} = 1$ TeV. Both cases correspond to the square root ansatz of eqn. (42) with a negative relative sign.

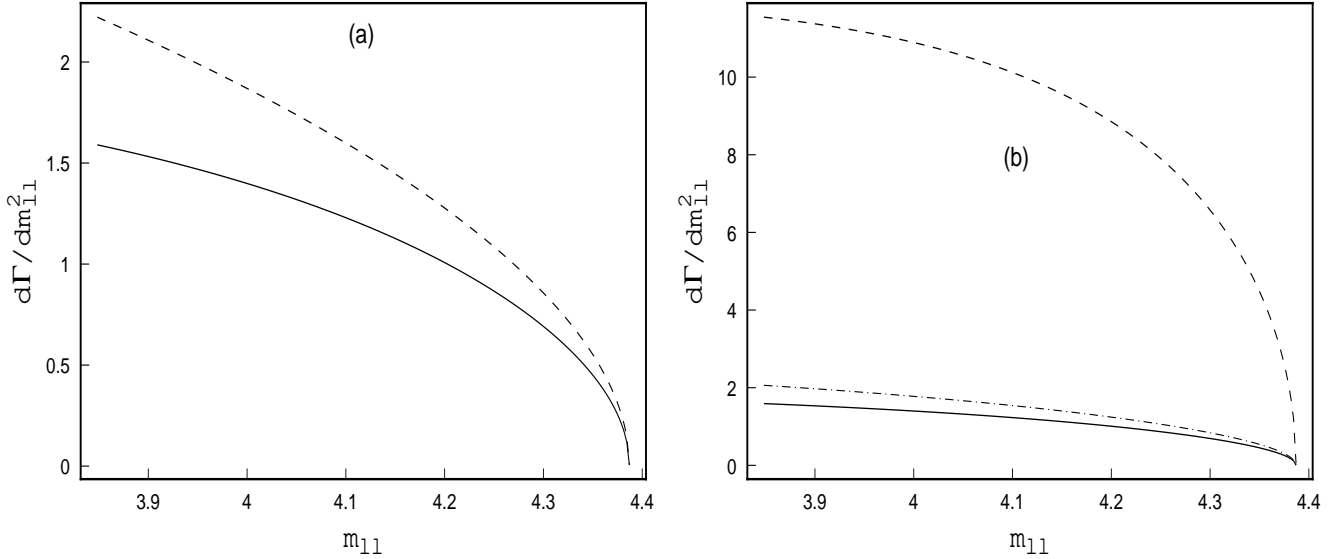


FIG. 3. Dilepton mass distributions for $B \rightarrow K^* \ell^+ \ell^-$. The caption is the same as in Fig. 2.

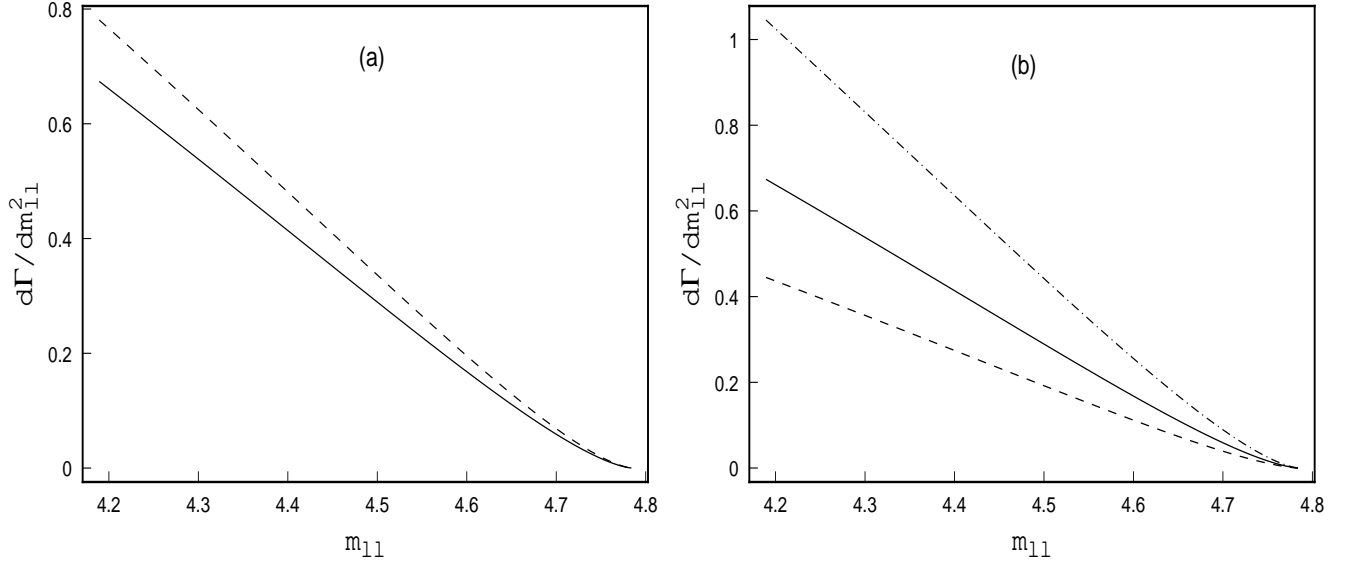


FIG. 4. Dilepton mass distributions in $B \rightarrow K\ell^+\ell^-$. The caption is the same as in Fig. 2.

REFERENCES

- [1] M.S. Alam *et al.*, CLEO collaboration, Phys. Rev. Lett. **74**, 2885 (1995).
- [2] S. Bertolini, F. Borzumati, A. Masiero and G. Ridolfi, Nucl. Phys. **B353**, 591 (1991);
V. Barger, M. S. Berger and R. J. N. Phillips, Phys. Rev. Lett. **70**, 1368 (1993);
J. Hewett, Phys. Rev. Lett. **70**, 1045 (1993); also in SCLAC-PUB-6521, presented at
the SLAC Summer Institute on Particle Physics, SLAC, Jul 6 - Aug 6, 1993.
- [3] N. Isgur and M. B. Wise, Phys. Rev. **D42**, 2388 (1990).
- [4] P. Avery *et al.*, CLEO collaboration, Phys. Lett. **B223**, 470 (1989); R. Balest *et al.*,
CLEO collaboration, CLEO-CONF-94-4, submitted to the Glasgow meeting, ICHEP94.
- [5] C. Anway-Wiese, CDF collaboration, Fermilab-Conf-94/210-E, to appear in the pro-
ceeding of the 1994 DPF Meeting, Albuquerque, New Mexico 1994.
- [6] A. Ali, T. Mannel and T. Morozumi, Phys. Lett. **B273**, 505 (1991); A. Ali, G. F.
Giudice and T. Mannel, CERN-TH.7346/94.
- [7] C. Greub, A. Ioannissian and D. Wyler, Phys. Lett. **B346**, 149 (1995); G. Baillie,
Z.Phys. **C61**, 667 (1994)
- [8] D. Liu, Phys. Lett. **B346**, 355 (1995).
- [9] C. T. Hill, Phys. Lett. **B345**, 483 (1995).
- [10] B. Grinstein, M. J. Savage and M. B. Wise, Nucl. Phys. **B319**, 271 (1989).
- [11] B. Grinstein, R. Springer and M. B. Wise, Nucl. Phys. **B339**, 269 (1990).
- [12] A. J. Buras, M. Misiak, M. Münz and S. Pokorski, Nucl. Phys. **B424**, 374 (1994);
M. Ciuchini, E. Franco, G. Martinelli, L. Reina and L. Silvestrini, Phys. Lett. **B316**,
127 (1993); M. Ciuchini, E. Franco, L. Reina and L. Silvestrini, Nucl. Phys. **B421**, 41
(1994).
- [13] A. J. Buras and M. Münz, Technische Universität München preprint TUM-T31-82/94.
- [14] A. Falk, M. Luke and M. Savage, Phys. Rev. **D49**, 3367 (1994).
- [15] G. Burdman and J.F. Donoghue, Phys. Lett. **B270**, 55 (1991).
- [16] L. Gibbons, CLEO collaboration, talk delivered at the Moriond meeting, March 1995.
- [17] R. J. Morrison and J. D. Richman in Particle Data Group, Phys. Rev. **D50**, 1565
(1994).
- [18] T. Inami and C. S. Lim, Progr. Theor. Phys. **65**, 297 (1981).
- [19] G. Burdman, in preparation.
- [20] C. T. Hill and S. J. Parke, Phys. Rev. **D49**, 4454 (1994).
- [21] C. T. Hill and X. Zhang, Phys. Rev. **D51**, 3563 (1994).